

# The Phase-Shift Method for the Langmuir Adsorption Isotherms of Electroadsorbed Hydrogens for the Cathodic H<sub>2</sub> Evolution Reactions at the Poly-Pt Electrode Interfaces

Jang H. Chun<sup>†</sup>, Sang K. Jeon, and Jae H. Lee

Mission Technology Research Center, Department of Electronic Engineering, Kwangwoon University, Seoul 139-701, Korea

(Received May 15, 2002; Accepted June 27, 2002)

**Abstract.** The Langmuir adsorption isotherms of the under-potentially deposited hydrogen (UPD H) and the over-potentially deposited hydrogen (OPD H) at the poly-Pt/0.5 M H<sub>2</sub>SO<sub>4</sub> and 0.5 M LiOH aqueous electrolyte interfaces have been studied using cyclic voltammetric and ac impedance techniques. The behavior of the phase shift ( $0^\circ \leq -\phi \leq 90^\circ$ ) for the optimum intermediate frequency corresponds well to that of the fractional surface coverage ( $1 \geq \theta \geq 0$ ) at the interfaces. The phase-shift method, i.e., the phase-shift profile ( $-\phi$  vs.  $E$ ) for the optimum intermediate frequency, can be used as a new electrochemical method to determine the Langmuir adsorption isotherms ( $\theta$  vs.  $E$ ) of the UPD H and the OPD H for the cathodic H<sub>2</sub> evolution reactions at the interfaces. At the poly-Pt/0.5 M H<sub>2</sub>SO<sub>4</sub> aqueous electrolyte interface, the equilibrium constant ( $K$ ) and the standard free energy ( $\Delta G_{ads}$ ) of the OPD H are  $2.1 \times 10^{-4}$  and 21.0 kJ/mol, respectively. At the poly-Pt/0.5 M LiOH aqueous electrolyte interface,  $K$  transits from 2.7 (UPD H) to  $6.2 \times 10^{-6}$  (OPD H) depending on the cathode potential ( $E$ ) and vice versa. Similarly,  $\Delta G_{ads}$  transits from -2.5 kJ/mol (UPD H) to 29.7 kJ/mol (OPD H) depending on  $E$  and vice versa. The transition of  $K$  and  $\Delta G_{ads}$  is attributed to the two distinct adsorption sites of the UPD H and the OPD H on the poly-Pt surface. The UPD H and the OPD H on the poly-Pt surface are the independent processes depending on the H adsorption sites themselves rather than the sequential processes for the cathodic H<sub>2</sub> evolution reactions. The criterion of the UPD H and the OPD H is the H adsorption sites and processes rather than the H<sub>2</sub> evolution reactions and potentials. The poly-Pt wire electrode is more efficient and useful than the Pt(100) disc electrode for the cathodic H<sub>2</sub> evolution reactions in the aqueous electrolytes. The phase-shift method is well complementary to the thermodynamic method rather than conflicting.

**초 록 :** 순환전압전류 및 교류임피던스 기법을 이용하여 다결정 Pt/0.5 M H<sub>2</sub>SO<sub>4</sub> 및 0.5 M LiOH 수용액 계면에서 저전위 수소흡착(UPD H)과 과전위 수소흡착(OPD H)에 관한 Langmuir 흡착등온식( $\theta$  vs.  $E$ )을 연구조사 하였다. 계면에서 최적중간주파수일 때 위상이동( $0^\circ \leq -\phi \leq 90^\circ$ ) 거동은 표면피복율( $1 \geq \theta \geq 0$ ) 거동에 정확하게 상응한다. 위상이동 방법 즉 최적중간주파수일 때 위상이동 변화( $-\phi$  vs.  $E$ )는 계면에서 음극 H<sub>2</sub> 발생 반응에 관한 UPD H와 OPD H의 Langmuir 흡착등온식을 결정할 수 있는 새로운 전기화학적 방법으로 사용할 수 있다. 다결정 Pt/0.5 M H<sub>2</sub>SO<sub>4</sub> 수용액 계면에서 OPD H의 흡착평형상수( $K$ )와 표준자유에너지( $\Delta G_{ads}$ )는 각각  $2.1 \times 10^{-4}$ 와 21.0 kJ/mol 이다. 다결정 Pt/0.5 M LiOH 수용액 계면에서  $K$ 는 음전위( $E$ )에 따라 2.7 (UPD H)에서  $6.2 \times 10^{-6}$  (OPD H) 또는  $6.2 \times 10^{-6}$  (OPD H)에서 2.7 (UPD H)로 전이한다. 유사하게  $\Delta G_{ads}$ 는  $E$ 에 따라 -2.5 kJ/mol (UPD H)에서 29.7 kJ/mol (OPD H) 또는 29.7 kJ/mol (OPD H)에서 -2.5 kJ/mol (UPD H)로 전이한다.  $K$ 와  $\Delta G_{ads}$ 의 전이는 다결정 Pt 전극 표면의 상이한 UPD H와 OPD H의 흡착부위에 기인한다. 다결정 Pt 전극 계면에서 UPD H와 OPD H는 음극 H<sub>2</sub> 발생 반응에 따른 순차적 과정이 아니라, 수소 흡착부위 자체에 따른 독립적 과정이다. UPD H와 OPD H의 기준은 음극 H<sub>2</sub> 발생 반응과 전위가 아니라, 수소 흡착부위와 과정이다. 수용액에서 음극 H<sub>2</sub> 발생 반응에는 다결정 Pt 선 전극이 단결정 Pt(100) 원반 전극보다 더 효율적이고 유용하다. 위상이동 방법은 열역학적 방법과 상충적이지 않으나, 보완적이다.

**Key words :** Phase-shift method; Langmuir adsorption isotherm; Electroadsorbed hydrogen; Platinum electrodes

## 1. Introduction

The kinetics and mechanisms of electroadsorbed hydrogens at electrocatalytic metal (Pt, Rh, Pd, Ni, etc.)/aqueous electrolyte interfaces have been extensively studied in electrochemical hydrogen technologies.<sup>1-17)</sup> The under-potentially deposited hydrogen (UPD H) and the over-potentially deposited

hydrogen (OPD H) are necessary and important to understand the kinetics and mechanisms of the cathodic hydrogen (H<sub>2</sub>) evolution reactions (HER) at the electrocatalytic metal/aqueous electrolyte interfaces. Also, it is well known that the UPD H and the OPD H occupy different surface adsorption sites on the single-crystal faces and act as two distinguishable electroadsorbed H species while only the OPD H can contribute to the cathodic HER.<sup>1-17)</sup> Therefore, it is necessary to compare the costs and related parameters of the polycrystalline

<sup>†</sup>E-mail: jhchun@daisy.kwangwoon.ac.kr

and single-crystal electrodes for the cathodic HER under the same experimental conditions.

Many electrochemical methods and analyses on the H adsorption sites and processes for the cathodic HER at the electrocatalytic metal/aqueous electrolyte interfaces are described and reviewed elsewhere.<sup>1-8)</sup> The cyclic voltammetric and electrochemical impedance spectroscopic methods have been intensively used to study the cathodic HER at the interfaces. However, the relation, transition, and criterion of the UPD H and the OPD H at the electrocatalytic metal/aqueous electrolyte interfaces have been studied from the point of view of the HER and potentials rather than the H adsorption sites and processes, i.e., the Langmuir or the Frumkin adsorption isotherms.

The Langmuir adsorption isotherm has all the ingredients of equations of the kinetics and thermodynamics.<sup>18)</sup> It is well known that the Langmuir adsorption isotherm is a special case of the Frumkin adsorption isotherm. The Langmuir adsorption isotherm can be derived from the Frumkin adsorption isotherm by setting the interaction parameter is zero. Although the Langmuir adsorption isotherm may be regarded a classical model and theory in physical electrochemistry, it is useful and effective to study the adsorption sites of the UPD H and the OPD H and processes for the cathodic HER at the interfaces. Thus, there is a technological need for a fast, simple, and reliable technique to estimate or determine the Langmuir adsorption isotherms for characterizing the relation, transition, and criterion between the UPD H and the OPD H for the cathodic HER at the interfaces.

Recently, we have experimentally and consistently found that the phase-shift profile for the optimum intermediate frequency, i.e., the phase-shift method, can be used to determine the Langmuir or the Frumkin adsorption isotherms of the UPD H and the OPD H for the cathodic HER at the electrocatalytic metal (Pt, Ir, Pd, Au, Ni)/aqueous electrolyte interfaces.<sup>19-26)</sup> It is useful and easy for studying the electrode kinetics and thermodynamics, the relation, transition, and criterion between the UPD H and the OPD H for the cathodic HER at the electrocatalytic metal/aqueous electrolyte interfaces.

In this paper we will propose the phase-shift method for the Langmuir adsorption isotherm and represent the relation, transition, and criterion between the UPD H and the OPD H for the cathodic HER at the poly-Pt/0.5 M H<sub>2</sub>SO<sub>4</sub> and 0.5 M LiOH aqueous electrolyte interfaces. It is complementary to the Langmuir adsorption isotherms of electroadsorbed hydrogens for the cathodic HER at the poly-Pt wire<sup>20,22)</sup> and the Pt(100) disc<sup>23)</sup> electrode interfaces. It appears that the phase-shift method is useful and necessary to determine or estimate the Langmuir adsorption isotherm and to compare and select an efficient electrode for the cathodic HER at the interfaces.

## 2. Experimental

### 2.1. Preparations

Taking into account H<sup>+</sup> concentrations and effects of diffuse double layer and pH,<sup>27)</sup> acidic and alkaline aqueous

electrolytes were prepared from H<sub>2</sub>SO<sub>4</sub> (Junsei, special grade) and LiOH (Alfa Aesar, Johnson Matthey, purity: 98%) with purified water (resistivity: > 18 MΩ cm) obtained from a Millipore system. The 0.5 M H<sub>2</sub>SO<sub>4</sub> and 0.5 M LiOH aqueous electrolytes were deaerated with 99.999% purified nitrogen gas for 10 min before the experiments.

A standard 3-electrode configuration was employed using an SCE (Saturated Calomel Electrode) reference electrode and a poly-Pt wire (Johnson Matthey, purity: 99.9985%, 1 mm diameter, estimated surface area: ~1 cm<sup>2</sup>) working electrode. In contrast to the Pt(100) disc,<sup>23)</sup> which was commercially prepared using the mechanical polishing, the poly-Pt wire was prepared by flame cleaning and then quenched and cooled in the Millipore Milli-Q water and in air, sequentially. A Pt wire (Johnson Matthey, purity: 99.95%, 1.5 mm diameter) was used as a counter electrode. Taking into account the OPD H and its large current distribution,<sup>28)</sup> the working and counter electrodes were separately placed (~4 cm) in the same compartment of a Pyrex cell using Teflon holders.

### 2.2. Measurements

Cyclic voltammetric (scan potential: -0.24 to 1.25 V vs. SCE, scan rate: 300 mV/s for the 0.5 M H<sub>2</sub>SO<sub>4</sub> and scan potential: 0 to -0.90 V vs. SCE, scan rate: 300 mV/s for the 0.5 M LiOH) and ac impedance (single sine wave, scan frequency: 10<sup>4</sup> to 1 Hz, ac amplitude: 5 mV, dc potential: 0 to -0.45 V vs. SCE for the 0.5 M H<sub>2</sub>SO<sub>4</sub> and to -1.35 V vs. SCE for the 0.5 M LiOH) techniques were used to study the relation between the phase-shift profile for the optimum intermediate frequency and the corresponding Langmuir adsorption isotherm. The high scan rate (> 100 mV/s) was used to measure the state of the poly-Pt working electrode at the commencement of the cyclic scan.<sup>28)</sup>

The cyclic voltammetric experiment was performed using an EG&G PAR Model 273A potentiostat controlled with the PAR Model 270 software package. The ac impedance experiment was performed using the same apparatus in conjunction with a Schlumberger SI 1255 HF Frequency Response Analyzer controlled with the PAR Model 388 software package. In order to obtain comparable and reproducible results, all measurements were carried out using the same preparations, procedures, and conditions at room temperature. The international sign convention is used, i.e., cathodic currents and lagged phase shifts or angles are taken as negative. Finally, in order to clarify the hydrogen adsorption in the different aqueous electrolytes, all potentials in the text, the Figures, and the Tables are given on the RHE (Reversible Hydrogen Electrode) scale.

## 3. Results and Discussion

### 3.1. Under-potentially deposited hydrogen (UPD H) peak

Figure 1 shows the cyclic voltammogram of the steady state at the poly-Pt/0.5 M H<sub>2</sub>SO<sub>4</sub> aqueous electrolyte interface. The UPD H peaks occur at ca. 0.215 and 0.077 V vs. RHE. The anionic adsorption effects, which are not serious for the

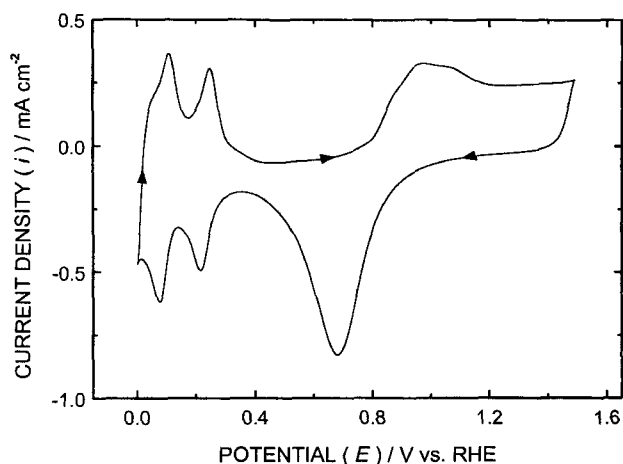


Fig. 1. The typical cyclic voltammogram at the poly-Pt/0.5 M H<sub>2</sub>SO<sub>4</sub> aqueous electrolyte interface. Estimated surface area: ~1 cm<sup>2</sup>. Scan potential: 0 to 1.49 V vs. RHE. Scan rate: 300 mV/s. 20th scan.

adsorption process of the OPD H, on the UPD H peaks have not been considered.<sup>7,17)</sup> Fig. 1 also shows that the cyclic voltammogram of the poly-Pt/0.5 M H<sub>2</sub>SO<sub>4</sub> aqueous electrolyte interface is similar to that of the Pt(100)/0.5 M H<sub>2</sub>SO<sub>4</sub>,<sup>23)</sup> the Pt(100)/0.3 M HF,<sup>29)</sup> or the H<sub>1</sub>-Pt/0.5 M H<sub>2</sub>SO<sub>4</sub> aqueous electrolyte interface.<sup>30)</sup> However, the shape of the cyclic voltammogram of the poly-Pt electrode is different from that of the Pt(100) electrodes which were prepared by the flame annealing method.<sup>8,15,17,31-34)</sup> It implies that the preparation of the poly-Pt wire, as well as the commercially prepared Pt (100) discs,<sup>23,29)</sup> is effective rather than perfect. In other words, the various UPD H peaks correspond to the adsorptions of H on the different single-crystal faces, e.g., (100), (110), (111), etc., which are attributed to imperfections in the orientation of the single-crystal substrates.<sup>30,33-35)</sup> Also, it implies that the activities of the adsorption sites of the UPD H and the OPD H depend strongly on the different single-crystal faces themselves rather than the sizes and/or the orientations of the same single-crystal faces on the poly-Pt electrode surface. However, the difference of the electrode kinetic and thermodynamic parameters between the poly-Pt wire and the Pt(100) disc<sup>23)</sup> electrodes is negligible (Table 3). It is understood that the poly-Pt wire mostly consists of the same single-crystal face (100) substrates.

The UPD H peaks and the corresponding cathode potentials are necessary and useful to verify the Langmuir adsorption isotherms of the UPD H and the OPD H for the cathodic HER at the interface. This is discussed in more detail later.

### 3.2. Phase-shift profile for the optimum intermediate frequency

Various equivalent circuits were proposed to model the frequency responses of the interfaces for intermediate adsorptions under different conditions.<sup>10,14,36-41)</sup> The equivalent circuit for the cathodic HER is usually expressed as shown in Fig. 2(a).<sup>10,14,36,39,41)</sup> Taking into account the relaxation time effect which is inevitable under the ac impedance experiment,<sup>10,42)</sup> the equivalent circuit elements shown in Fig. 2(a) are defined

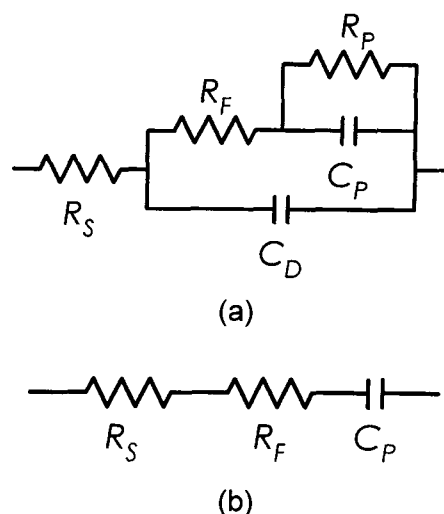


Fig. 2. (a) The equivalent circuit for the cathodic H<sub>2</sub> evolution reactions at the poly-Pt/0.5 M H<sub>2</sub>SO<sub>4</sub> and 0.5 M LiOH aqueous electrolyte interfaces and (b) The simplified equivalent circuit for the intermediate frequencies at the interfaces.

as:  $R_S$  is the electrolyte resistance,  $R_F$  is the equivalent resistance due to the adsorption process of H (UPD H, OPD H) and its relaxation time effect at the interface,  $R_P$  is the equivalent resistance due to the recombination reaction,  $C_P$  is the equivalent capacitance due to the adsorption process of H (UPD H, OPD H) and its relaxation time effect at the interface, and  $C_D$  is the double-layer capacitance. The impedance ( $Z$ ) of the equivalent circuit shown in Fig. 2(a) is given by:<sup>36)</sup>

$$Z = R_S + \left\{ (R_F + R_P + j\omega R_F R_P C_P) / [1 - \omega^2 R_F R_P C_P C_D + j\omega (R_P C_P + R_F C_D + R_P C_D)] \right\} \quad (1)$$

where  $j$  is an operator and is equal to the square root of -1, i.e.,  $j^2 = -1$ , and  $\omega (= 2\pi f)$  is the angular frequency.

The two equivalent circuit elements, i.e.,  $R_F$  and  $C_P$  are the equivalent resistance and capacitance associated with the faradaic resistance ( $R_\phi$ ) and the adsorption pseudocapacitance ( $C_\phi$ ) of the UPD H and/or the OPD H, respectively. Under the ac impedance experiment,  $R_F$  is smaller than  $R_\phi$  due to the relaxation times of the previously adsorbed H, i.e., the increase of H<sup>+</sup> on the electrode surface. On the other hand,  $C_P$  is greater than  $C_\phi$  due to the relaxation times of the previously adsorbed H, i.e., the increase of H<sup>+</sup> on the electrode surface. Since, in general, a resistance is inversely proportional to charged species but a capacitance is proportional to charged species on the electrode surface. It implies that the relaxation time effects of  $R_F$  and  $C_P$  can be cancelled out or compensated together. This is discussed in more detail later.

Essentially, both the relaxation time and lateral interaction effects at the interfaces are proportional to the fractional surface coverage ( $\theta$ ) of the UPD H and/or the OPD H. It implies that the behaviors of  $R_F$  and  $C_P$  depend strongly on those of  $R_\phi$  and  $C_\phi$ . Also, it implies that the lateral interaction effect depends strongly on  $R_F$  and  $C_P$  i.e.,  $R_\phi$  and  $C_\phi$  or  $\theta$ . Therefore, the adsorption process of the UPD H and/or the OPD H

corresponding to the combination of  $R_F$  and  $C_P$  can be correctly expressed in terms of the phase delay. This aspect was not well interpreted in the previously published papers.<sup>19-22</sup> Of course, the experimental results presented there and related discussions are unchanged. However, it is well known that the fractional surface coverage depends on the applied dc potential at the interfaces. Also, it is well known that the phase shift or angle depends on the applied dc potential at the interfaces. At present, it is difficult to derive the theoretical relation between the phase shift and the fractional surface coverage at the interfaces.<sup>26)</sup>

The frequency responses of the equivalent circuit shown in Fig. 2(a) are important and useful to study the relationship between the phase shift and the fractional surface coverage for the cathodic HER at the interfaces. At low frequencies, the equivalent circuit can be expressed as a series circuit of  $R_S$ ,  $R_F$ , and  $R_P$ . At high frequencies, the equivalent circuit can be expressed as a series circuit of  $R_S$  and  $C_D$ . At intermediate frequencies, the equivalent circuit can be simplified as a series circuit of  $R_S$ ,  $R_F$ , and  $C_P$  shown in Fig. 2(b).<sup>36)</sup> In practice,  $R_P$  is much greater than  $R_F$ . Also,  $C_P$  is much greater than  $C_D$  except at  $\theta=0$ . In addition,  $|R_P|$  is much greater than  $|1/\omega C_P|$  for the intermediate frequencies. Therefore,  $R_P$  and  $C_D$  can be eliminated from the equivalent circuit for the cathodic HER shown in Fig. 2(a). It implies that the simplified equivalent circuit for the intermediate frequencies shown in Fig. 2(b) can be applied to the poly-Pt/0.5 M  $H_2SO_4$  and 0.5 M LiOH electrolyte interfaces regardless of  $H_2$  evolution. However, it should be noted that the simplified equivalent circuit shown in Fig. 2(b) is not change of the cathodic HER itself but only the intermediate frequency response itself. In other words, it is valid and effective for studying the UPD H and/or the OPD H at the interfaces. The frequency responses of the equivalent circuit shown in Fig. 2(a) are described elsewhere.<sup>36-41)</sup>

The impedance ( $Z$ ) of the equivalent circuit for the intermediate frequencies shown in Fig. 2(b) and the corresponding phase shift ( $\phi$ ) or angle are given by:<sup>43)</sup>

$$Z = (R_S + R_F) - j/\omega C_P \quad (2)$$

$$\phi = -\tan^{-1}[1/\omega(R_S + R_F)C_P] \quad (3)$$

$$R_F \propto R_\phi (< R_\phi), R_F > R_S, C_P > C_D, \text{ and } C_P \propto C_\phi (> C_\phi) \quad (4)$$

where  $R_\phi$  is the faradaic resistance for the discharge reaction of the UPD H or the OPD H and depends on the fractional surface coverage ( $\theta$ ) of the UPD H or the OPD H, and  $C_\phi$  is the adsorption pseudocapacitance and also depends on  $\theta$  of the UPD H or the OPD H.<sup>36)</sup> It should be noted that both  $R_\phi$  (or  $R_F$ ) and  $C_\phi$  (or  $C_P$ ) cannot exist unless charge is transferred across the interphase.

A minus sign shown in Eq. (3) implies a lagged phase. In practice, the value of  $R_S$  at the poly-Pt/0.5 M  $H_2SO_4$  aqueous electrolyte interface is  $\sim 1.1$ - $1.4 \Omega \text{ cm}^2$  which can be neglected comparing to that of  $R_F$  (Fig. 3). Therefore, from Eq. (3), it is readily understood that the lagged phase depends strongly

on  $R_F$  and  $C_P$  i.e.,  $R_\phi$  and  $C_\phi$  or  $\theta$ . It was pointed out by Gileadi and Conway<sup>18,44)</sup> that the shape of the  $C_\phi$  vs.  $E$  is the exact form of the  $\theta$  vs.  $E$ . It implies that the lagged phase shift ( $-\phi$ ) also depends markedly on the adsorption process of the UPD H and/or the OPD H at the interface. However, as previously described, it should not be confused  $C_P$  with  $C_\phi$  which has a maximum value at  $\theta=0.5$  and can be neglected at  $\theta=0$  and 1.<sup>10,23,36,39,40)</sup> Also, it should not be confused that the simplified equivalent circuit shown in Fig. 2(b) is not change of the cathodic HER itself but only the intermediate frequency response itself. Consequently, it is understood that the simplified equivalent circuit for the intermediate frequencies is effective and valid to determine the Langmuir adsorption isotherm for the cathodic HER.

Figures 3(a) and (b) show the profiles of the measured  $R_F$  and  $C_P$  versus the cathode potential ( $E$ ) for the optimum intermediate frequency (ca. 3 Hz) at the poly-Pt/0.5 M  $H_2SO_4$  aqueous electrolyte interface, respectively. As previously described, Fig. 3(a) shows that  $R_F$  is smaller than  $R_\phi$ . Since, the left-hand side of the profile ( $R_F$  vs.  $E$ ) is lower than the right-hand side of the profile. It is attributed to the superposition of the Langmuir adsorption process and the relaxation time effect of  $R_F$ , and the nature of resistance which is inversely proportional to charged species. On the other hand, as previously described, Fig. 3(b) shows that  $C_P$  is greater than  $C_\phi$ . Since, the profile ( $C_P$  vs.  $E$ ) increases from the right-hand side to the left-hand side, i.e., towards more negative potentials. Similarly, it is attributed to the superposition of the Langmuir adsorption process and the relaxation time effect of  $C_P$  and the nature of capacitance which is proportional to charged species. However, it should be noted that the equivalent resistance profile ( $R_F$  vs.  $E$ ) shown in Fig. 3(a)

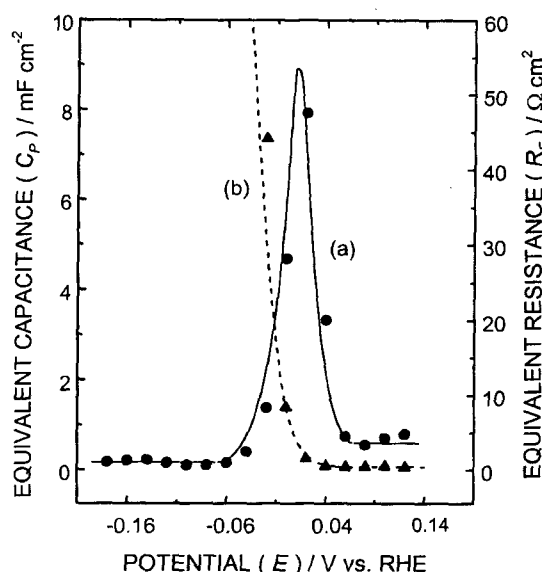


Fig. 3. The profiles of the measured equivalent circuit elements ( $R_F$ ,  $C_P$ ) versus  $E$  for the optimum intermediate frequency (ca. 3 Hz) at the poly-Pt/0.5 M  $H_2SO_4$  aqueous electrolyte interface. Single sine wave. Scan frequency:  $10^4$  to 1 Hz. ac amplitude: 5 mV. dc potential: 0.14 to -0.18 V vs. RHE. (a) Equivalent resistance profile ( $R_F$  vs.  $E$ ) and (b) Equivalent capacitance profile ( $C_P$  vs.  $E$ ).

has the peak due to the Langmuir adsorption process. On the other hand, the equivalent capacitance profile ( $C_p$  vs.  $E$ ) shown in Fig. 3(b) has not the peak. It implies that the  $H^+$  at the interface increases consistently with increase of the applied dc potential, i.e., the cathode potential ( $E$ ). As previously described, it is attributed to the superposition of the Langmuir adsorption process and the relaxation time effect, and the reciprocal nature between the resistance and the capacitance at the interface. It also implies that the relaxation time effects of  $R_F$  and  $C_p$  depend strongly on  $\theta$ . However, it should be noted that Fig. 3(b) shows that  $C_p$  increases rapidly beyond the peak potential (ca. 0 V vs. RHE) of the equivalent resistance profile ( $R_F$  vs.  $E$ ). It is understood that  $C_p$  has a maximum value at the peak potential, i.e.,  $\theta = 0.5$ , due to the Langmuir adsorption process. The determination of the optimum intermediate frequency is discussed in more detail later. Consequently, it can be interpreted that the relaxation time effects of  $R_F$  and  $C_p$  are the useful and unique feature to analyze the adsorption process of H at the poly-Pt/0.5 M  $H_2SO_4$  aqueous electrolyte interface. The lateral interaction effect of the Langmuir adsorption process is negligible at the interface.

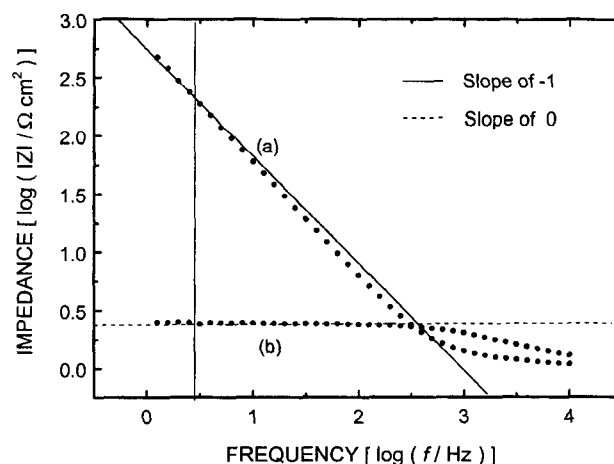
From Figs. 2(b), 3, and Eq. (3), it is understood that the real surface area problem of the poly-Pt electrode is not important or serious to study the phase-shift profile. Since, the real surface area effects of  $R_F$  and  $C_p$  are completely cancelled out or compensated together. Also, it is understood that the adsorption process of H at the interface can be expressed in terms of the lagged phase. In practice,  $R_F$  is greater than  $R_s$  and so the lagged phase shift ( $-\phi$ ) can be substantially determined by the series circuit of  $R_F$  and  $C_p$ . In other words,  $-\phi$  is substantially characterized by the series circuit of  $R_\phi$  and  $C_\phi$  or  $\theta$ , i.e., the adsorption process of the UPD H and/or the OPD H. It implies that the behavior of the phase shift ( $0^\circ \leq -\phi \leq 90^\circ$ ) for the optimum intermediate frequency can be related to that of the fractional surface coverage ( $1 \geq \theta \geq 0$ ). It also implies that the change rate of  $\Delta(-\phi)/\Delta E$  or  $d(-\phi)/dE$  corresponds well to that of  $\Delta\theta/\Delta E$  or  $d\theta/dE$  (Fig. 7). This is discussed in more detail later. However, it appears that the mathematical relation between the phase shift ( $-\phi$ ) and the fractional surface coverage ( $\theta$ ) has not been derived or reported elsewhere.

Figure 4 shows the comparison of the two clearly distinguishable frequency responses at the poly-Pt/0.5 M  $H_2SO_4$  aqueous electrolyte interface. The absolute value of the impedance vs. the frequency ( $|Z|$  vs.  $f$ ) is plotted on a log-log scale. In Fig. 4(a), the slope portion of the frequency response curve represents the capacitive behavior of the poly-Pt/0.5 M  $H_2SO_4$  aqueous electrolyte interface. Since, a slope of -1 represents the ideal capacitive behavior. It implies that the Langmuir adsorption process of H and its relaxation time effect at the interface are minimized. In other words,  $\theta$  can be set to zero as shown in Table 1. Therefore, from Eq. (3),  $-\phi$  has a maximum value ( $\leq 90^\circ$ ) as shown in Fig. 5(a). On the other hand, in Fig. 4(b), the horizontal portion of the frequency response curve represents the resistive behavior of the poly-Pt/0.5 M  $H_2SO_4$  aqueous electrolyte interface. Since, a slope of zero represents the ideal resistive behavior. It

**Table 1.** The measured phase shift ( $-\phi$ ) for the optimum intermediate frequency (ca. 3 Hz) and the estimated fractional surface coverage ( $\theta$ ) at the poly-Pt/0.5 M  $H_2SO_4$  aqueous electrolyte interface

$E$ (V vs. RHE)	$-\phi$ (deg)	$\theta^a$
0.08	88.6	$\approx 0$
0.06	88.3	0.003
0.04	83.3	0.060
0.02	66.3	0.252
0.00	46.8	0.473
-0.02	34.9	0.607
-0.04	23.0	0.742
-0.06	11.2	0.876
-0.08	5.2	0.943
-0.10	3.1	0.967
-0.12	1.7	0.983
-0.14	0.8	0.993
-0.16	0.3	0.999
-0.18	0.2	$\approx 1$

<sup>a</sup> Estimated using the measured phase shift ( $-\phi$ ).



**Fig. 4.** The comparison of the two extremely distinguishable frequency response curves at the poly-Pt/0.5 M  $H_2SO_4$  aqueous electrolyte interface. Vertical solid line: ca. 3 Hz. Single sine wave. Scan frequency:  $10^4$  to 1 Hz. ac amplitude: 5 mV. dc potential: (a) 0.08 V and (b) -0.18 V vs. RHE.

implies that the Langmuir adsorption process of H and its relaxation time effect at the interface are maximized or almost saturated. In other words,  $\theta$  of the OPD H can be set to unity as shown in Table 1.<sup>6)</sup> Therefore, from Eq. (3),  $-\phi$  has a minimum value ( $\geq 0^\circ$ ) as shown in Fig. 5(e).

Figure 5 shows the comparison of the phase-shift curves ( $-\phi$  vs.  $f$ ) for the different cathode potentials at the poly-Pt/0.5 M  $H_2SO_4$  aqueous electrolyte interface. In Fig. 5, it should be noted that the lagged phase shifts or angles and related phase-shift curves are markedly characterized at the intermediate frequencies. The low side (ca. 3 Hz) of a slope of 1 shown in Fig. 4(a), i.e., the low side of the intermediate fre-

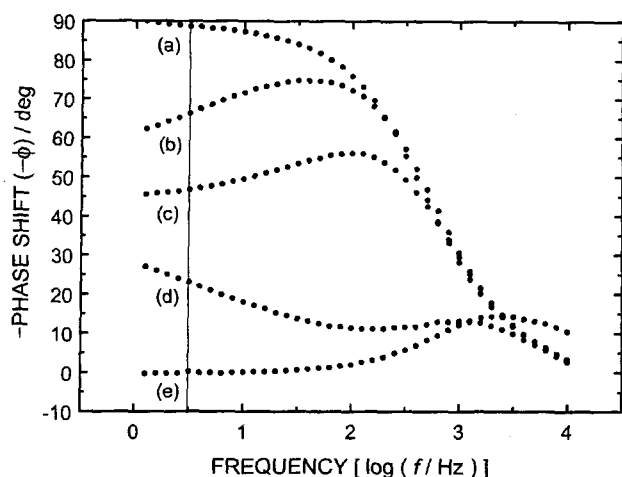


Fig. 5. The comparison of the phase-shift curves at the poly-Pt/0.5 M H<sub>2</sub>SO<sub>4</sub> aqueous electrolyte interface. Vertical solid line: ca. 3 Hz. Single sine wave. Scan frequency: 10<sup>4</sup> to 1 Hz. ac amplitude: 5 mV. dc potential: (a) 0.08 V, (b) 0.02 V, (c) 0 V, (d) -0.04 V, and (e) -0.18 V vs. RHE.

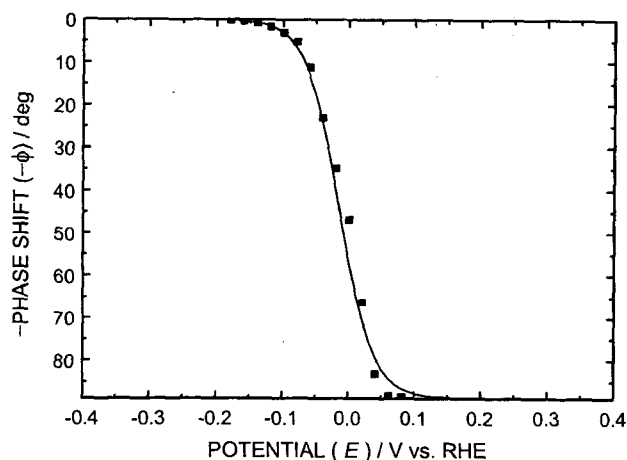


Fig. 6. The phase-shift profile ( $-\phi$  vs.  $E$ ) for the optimum intermediate frequency (ca. 3 Hz) at the poly-Pt/0.5 M H<sub>2</sub>SO<sub>4</sub> aqueous electrolyte interface.

frequencies (ca. 1-10 Hz), can be set as the optimum intermediate frequency for the phase-shift profile ( $-\phi$  vs.  $E$ ). Of course, the exactly same shape of the phase-shift profile can also be obtained at ca. 1 and 10 Hz, i.e., the range of the intermediate frequencies. The determination of the optimum intermediate frequency for the phase-shift profile is described elsewhere.<sup>19-26</sup> Finally, the cathode potentials and the corresponding phase shifts for the optimum intermediate frequency (ca. 3 Hz) can be plotted as the phase-shift profile ( $-\phi$  vs.  $E$ ) shown in Fig. 6.

As shown in Fig. 3, the relaxation time effects of  $R_F$  and  $C_P$  are very small or negligible for the range of  $\theta < 0.5$ , i.e., the right-hand side of the profile ( $R_F$  vs.  $E$  or  $C_P$  vs.  $E$ ) shown in Fig. 3. It should be noted that the lateral interaction effect between the adsorbed OPD H is also negligible at the range of  $\theta < 0.5$ . Therefore, the shape of the phase-shift pro-

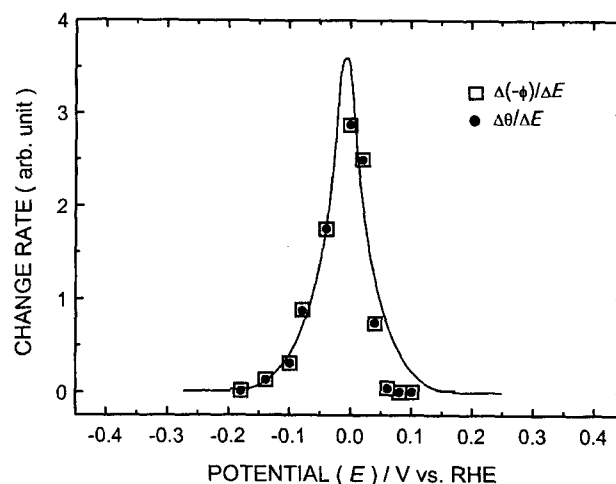


Fig. 7. The comparison of the change rates of the  $\Delta(-\phi)/\Delta E$  and the  $\Delta\theta/\Delta E$  for the optimum intermediate frequency (ca. 3 Hz) at the poly-Pt/0.5 M H<sub>2</sub>SO<sub>4</sub> aqueous electrolyte interface.

file ( $-\phi$  vs.  $E$ ) for the optimum intermediate frequency can be related to the form of the Langmuir adsorption isotherm ( $\theta$  vs.  $E$ ) at the interface. On the other hand, for the range of  $\theta \geq 0.5$ , the relaxation time effect at the interface should be considered as well as the lateral interaction effect. Since, as shown in Fig. 3, the relaxation time effects of  $R_F$  (or  $R_\phi$ ) and  $C_P$  (or  $C_\phi$ ) at the interface increase significantly with increasing of  $\theta$  ( $\geq 0.5$ ), i.e. beyond ca. 0 V vs. RHE. However, surprisingly, Figs. 6-8 show that the various effects and considerations, i.e., the intermediate frequency response and related equivalent circuit, the relaxation time effect, the lateral interaction effect, etc., are well supplemented and compensated together at the interface. Consequently, it can be interpreted that the form of the Langmuir adsorption isotherm ( $\theta$  vs.  $E$ ) is the exact shape of the phase-shift profile ( $-\phi$  vs.  $E$ ) for the optimum intermediate frequency. Both the relaxation time and lateral interaction effects on the Langmuir adsorption process are negligible at the interface.

Figure 7 shows the comparison of the change rates of the  $-\phi$  vs.  $E$  and the  $\theta$  vs.  $E$ , i.e., the  $\Delta(-\phi)/\Delta E$  or  $d(-\phi)/dE$  and the  $\Delta\theta/\Delta E$  or  $d\theta/dE$ , at the poly-Pt/0.5 M H<sub>2</sub>SO<sub>4</sub> aqueous electrolyte interface. The derivation of the  $\Delta(-\phi)/\Delta E$  and the  $\Delta\theta/\Delta E$  is based on the experimental data shown in Table 1. As expected, Table 1 and Fig. 7 show that both the  $\Delta(-\phi)/\Delta E$  or  $d(-\phi)/dE$  and the  $\Delta\theta/\Delta E$  or  $d\theta/dE$  are maximized at  $\theta \approx 0.5$  and are minimized at  $\theta = 0$  and 1. Fig. 7 also shows that the plot of the  $\Delta(-\phi)/\Delta E$  or  $d(-\phi)/dE$  is exactly same as that of the  $\Delta\theta/\Delta E$  or  $d\theta/dE$ . In other words, the behavior of the phase shift ( $0^\circ \leq -\phi \leq 90^\circ$ ) corresponds well to that of the fractional surface coverage ( $1 \geq \theta \geq 0$ ). Also, it should be noted that Fig. 7 is similar to the typical shape of the change rate of the adsorption pseudocapacitance ( $C_\phi$ ) for the Langmuir adsorption conditions.<sup>10,36,39,40</sup> As previously described, it implies that the relaxation time effects of  $R_F$  and  $C_P$ , the lateral interaction effect, etc., cannot be considered or are not conflicting to analyze the adsorption process of the UPD H and/or the OPD H at the interface. In other words, the lagged

phase shift ( $-\phi$ ) described in Eq. (3) depends strongly on  $R_\phi$  and  $C_\phi$ , i.e.,  $\theta$ . For the Frumkin adsorption process, both the  $\Delta(-\phi)/\Delta E$  or  $d(-\phi)/dE$  and the  $\Delta\theta/\Delta E$  or  $d\theta/dE$  will be changed depending on the interaction parameter.<sup>25,26</sup> Also, the peak will be changed as a plateau depending on the interaction parameter. Consequently, it can be interpreted that the shape of the phase-shift profile ( $-\phi$  vs.  $E$ ) for the optimum intermediate frequency corresponds well to the form of the Langmuir adsorption isotherm ( $\theta$  vs.  $E$ ) at the interface. Both the relaxation time and lateral interaction effects on the Langmuir adsorption process are negligible at the interface.

### 3.3. Langmuir adsorption isotherm

In electroadsorption, the electrode potential ( $E$ ) is introduced as an independent variable and affects the adsorption of charged species in a major way. Also, the electrode potential affects the adsorption of polar neutral molecules and neutral organic species having no permanent dipole moment.<sup>18,45</sup> Similarly, the Volmer, the Heyrovsky, and the Tafel reactions for the cathodic HER are considered at the poly-Pt/0.5 M  $H_2SO_4$  and 0.5 M LiOH aqueous electrolyte interfaces. However, the distinction between the Volmer, the Heyrovsky, and the Tafel reactions is not necessary and important. Since, as pointed out in Refs.,<sup>21,23,24</sup> the Langmuir adsorption isotherm corresponding to the phase-shift profile for the optimum intermediate frequency is strongly dependent on the adsorption sites of the UPD H and the OPD H rather than the sequential processes for the cathodic HER.

It is assumed that the UPD H and the OPD H for the cathodic HER are an equilibrium.<sup>46</sup> Since, the adsorption processes of the UPD H and the OPD H are very fast compared to the mass transport processes. However, from a viewpoint of change rate with respect to time, the electrical circuit elements at the steady state are equivalent to the electrode kinetic and thermodynamic parameters at the equilibrium. Therefore, taking into account the relaxation time effect on the ac impedance experiment and the overpotential for the cathodic HER at the interfaces, the state of the Langmuir adsorption isotherm corresponding to the phase-shift profile for the optimum intermediate frequency is considered as a quasi-equilibrium. Also, it should be noted that both the faradaic resistance and the adsorption pseudocapacitance occur at the quasi-equilibrium.<sup>36</sup> It cannot exist unless charge is transferred across the interphase.

At the Pt electrode interfaces, the consideration of the Langmuir adsorption isotherm for H is more preferable to discussion in terms of an equation of the kinetics and thermodynamics for H. Since, the Langmuir adsorption isotherm can be associated more directly with the atomic mechanism of H adsorption and is experimentally determined.<sup>18</sup>

The Langmuir adsorption isotherm is based on the assumptions that the surface is homogeneous and that the lateral interaction effect is negligible. The HER under the Langmuir adsorption conditions is described elsewhere.<sup>47</sup> Considering the application of the Langmuir adsorption isotherm to the adsorption of H on the poly-Pt electrode surface, the Langmuir adsorption isotherm at the quasi-equilibrium

can be expressed as follows:<sup>48</sup>

$$[\theta/(1 - \theta)] = KC_{H^+}[\exp(-EF/RT)] \quad (5)$$

where  $\theta$  is the fractional surface coverage of the UPD H or the OPD H,  $K$  is the equilibrium constant for the UPD H or the OPD H,  $C_{H^+}$  is the  $H^+$  concentration in the bulk electrolyte,  $E$  is the applied dc potential,  $F$  is the Faraday constant,  $R$  is the gas constant, and  $T$  is the absolute temperature. In Eq. (5), it should be noted that  $E$  is not the overpotential but the applied dc potential. The UPD H and the OPD H are a replacement reaction in which a number of water molecules are desorbed from the poly-Pt electrode surface, i.e., the adsorption sites of the UPD H and the OPD H, for each  $H^+$  adsorbed. In addition, as previously described, the fractional surface coverage ( $\theta$ ) of the OPD H for the cathodic HER approaches unity, i.e.,  $\theta \approx 1$ , at high negative overpotentials.<sup>23</sup>

Considering the adsorption sites on the different single-crystal faces<sup>4-8,13,15,16,29</sup> and the similar feature between the cyclic voltammograms shown in Fig. 1 and Refs.,<sup>23,29,30,34</sup> the poly-Pt wire, which mostly consists of the same single-crystal face (100) substrates, can also be considered as a homogeneous electrode. In other words, the imperfections in the orientation and size of the same single-crystal face (100) substrates are not serious for the Langmuir adsorption process. Therefore, it can be assumed that the poly-Pt electrode has the homogeneous surface. On the other hand, the oxide layer formations or the different single-crystal face substrates are serious for the Langmuir adsorption process and should be considered as a heterogeneous surface. In this case, the Temkin or the Frumkin adsorption process should be applied to the interface.<sup>18</sup>

As previously described, it is well known that the shape of the adsorption pseudocapacitance ( $C_\phi$  vs.  $E$ ) is the exact form of the Langmuir adsorption isotherm ( $\theta$  vs.  $E$ ).<sup>4,10,40,49,50</sup> However, it is based on the numerical simulation rather than the experimental data. For the Pt electrode interfaces,<sup>6</sup> it is also well known that  $\theta$  by the OPD H for the cathodic HER approaches unity, i.e.,  $\theta \approx 1$ , at high negative overpotentials as shown in Table 1. It implies that the  $\theta$  vs.  $E$  for the OPD H at the Pt electrode interface depends strongly on the fractional surface coverage ( $0 \leq \theta \leq 1$ ) rather than the lateral interaction effect. However, as previously described, the experimental results (Figs. 6 and 8) also show that the shape of the phase-shift profile for the optimum intermediate frequency is the exact form of the Langmuir adsorption isotherm. Consequently, it can be interpreted that the various definitions and considerations, i.e., the simplified equivalent circuit for the optimum intermediate frequency, the relaxation time effect, the quasi-equilibrium, the homogeneous surface, the lateral interaction effect, etc., are well supplemented and compensated together for the Langmuir adsorption isotherm at the interface.

At the poly-Pt/0.5 M  $H_2SO_4$  aqueous electrolyte (pH 0.62) interface, the fitted data, i.e., the numerically calculated Langmuir adsorption isotherm using Eq. (5), are shown in Fig. 8. As expected, the Langmuir adsorption isotherm ( $\theta$  vs.  $E$ )

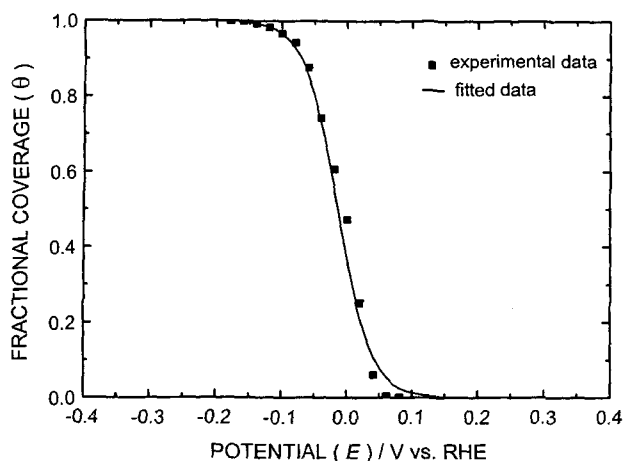


Fig. 8. The comparison of the experimental and fitted data for the Langmuir adsorption isotherm ( $\theta$  vs.  $E$ ) at the poly-Pt/0.5 M  $\text{H}_2\text{SO}_4$  aqueous electrolyte interface.  $K = 2.1 \times 10^{-4}$  (OPD H).

shown in Fig. 8 corresponds well to the phase-shift profile ( $-\phi$  vs.  $E$ ) for the optimum intermediate frequency shown in Fig. 6. From Fig. 8, it can be easily inferred that  $K = 2.1 \times 10^{-4}$  is applicable to the formation of H at the interface.

The Langmuir adsorption isotherm shown in Fig. 8 is attributed to the OPD H. As expected, the Langmuir adsorption isotherm due to the UPD H has not been observed at the cathode potential range. It is understood that the adsorption sites of the UPD H are almost masked due to a high  $\text{H}^+$  concentration of the 0.5 M  $\text{H}_2\text{SO}_4$  aqueous electrolyte and/or the anionic adsorption effects under the steady state conditions.<sup>7-9,12,13,15,17,21-24</sup> Also, it should be noted that the experimental data shown in Figs. 3-8 and Table 1 are observed beyond the UPD H peaks and the corresponding cathode potentials shown in Fig. 1. In other words, the Langmuir adsorption isotherm of the OPD H is located beyond that of the UPD H as shown in Figs. 11-13. Of course, the Langmuir adsorption isotherm of the UPD H can also be easily observed at the poly-Pt/alkaline aqueous electrolyte interface (Figs. 11 and 12). This is discussed in more detail later.

For the aqueous electrolytes, the standard free energy of H adsorption is given by the difference between the free energy of adsorption of H and that of a number of water molecules on the adsorption sites of the poly-Pt surface. Under the Langmuir adsorption conditions, the relation between the equilibrium constant ( $K$ ) for H adsorption (UPD H, OPD H) and the standard free energy ( $\Delta G_{ads}$ ) of H adsorption (UPD H, OPD H) is given using,<sup>48)</sup> as

$$2.3RT \log K = -\Delta G_{ads} \quad (6)$$

The definition of  $\Delta G_{ads}$  is described elsewhere.<sup>18,45)</sup> At the poly-Pt/0.5 M  $\text{H}_2\text{SO}_4$  aqueous electrolyte interface, it is readily calculated using Eq. (6) that  $\Delta G_{ads}$  is 21.0 kJ/mol for  $K = 2.1 \times 10^{-4}$  (OPD H). As expected, in contrast to the exothermic reaction, i.e.,  $\Delta G_{ads} < 0$ , at the UPD H region,<sup>6-8,12,13,15,21,23,49,50)</sup> the endothermic reaction, i.e.,  $\Delta G_{ads} > 0$ , occurs at the OPD H region of the poly-Pt electrode interface. It implies that the

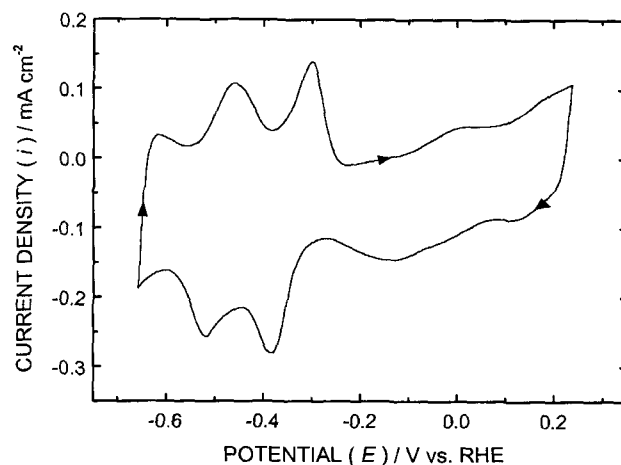


Fig. 9. The typical cyclic voltammogram at the poly-Pt/0.5 M LiOH aqueous electrolyte interface. Estimated surface area:  $\sim 1 \text{ cm}^2$ . Scan potential: 0.24 to -0.66 V vs. RHE. Scan rate: 300 mV/s. 20th scan.

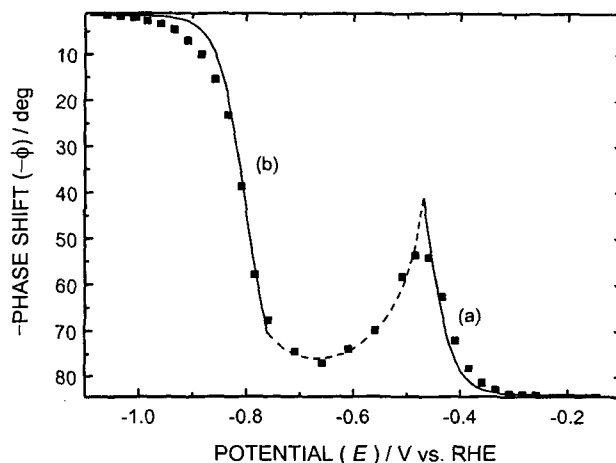


Fig. 10. The phase-shift profile ( $-\phi$  vs.  $E$ ) for the optimum intermediate frequency (ca. 13 Hz) at the poly-Pt/0.5 M LiOH aqueous electrolyte interface. (a) UPD H and (b) OPD H regions.

OPD H on the adsorption sites of the poly-Pt surface requires 21.0 kJ/mol to remove the appropriate number of water molecules. As shown in Fig. 8, 21.0 kJ/mol corresponds to the applied dc potentials, i.e., ca. 0.15 to -0.2 V vs. RHE.

#### 3.4. Transition between the UPD H and the OPD H

Figure 9 shows the cyclic voltammogram of the steady state at the poly-Pt/0.5 M LiOH aqueous electrolyte interface. The UPD H peaks occur at ca. -0.381 and -0.517 V vs. RHE. As previously described, the UPD H peaks and the corresponding cathode potentials are necessary and useful to verify the Langmuir adsorption isotherms of the UPD H and the OPD H for the cathodic HER at the interface.

Figures 10 and 11 show the phase-shift profile ( $-\phi$  vs.  $E$ ) for the optimum intermediate frequency (ca. 13 Hz) and the corresponding Langmuir adsorption isotherm ( $\theta$  vs.  $E$ ) at the poly-Pt/0.5 M LiOH aqueous electrolyte (pH 12.4) interface,



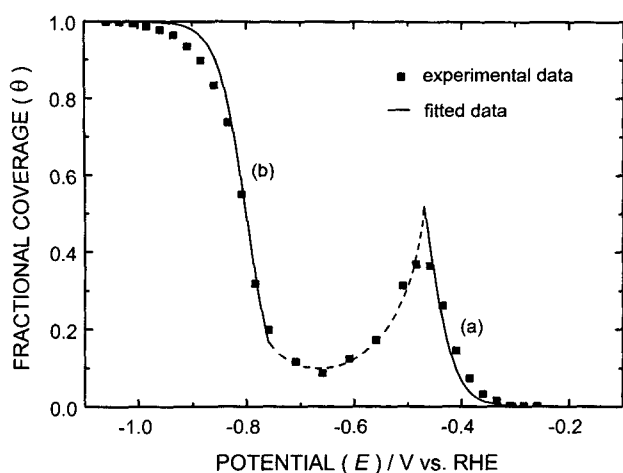


Fig. 11. The comparison of the experimental and fitted data for the Langmuir adsorption isotherm ( $\theta$  vs.  $E$ ) at the poly-Pt/0.5 M LiOH aqueous electrolyte interface. (a)  $K = 2.7$  (UPD H) and (b)  $K = 6.2 \times 10^{-6}$  (OPD H).

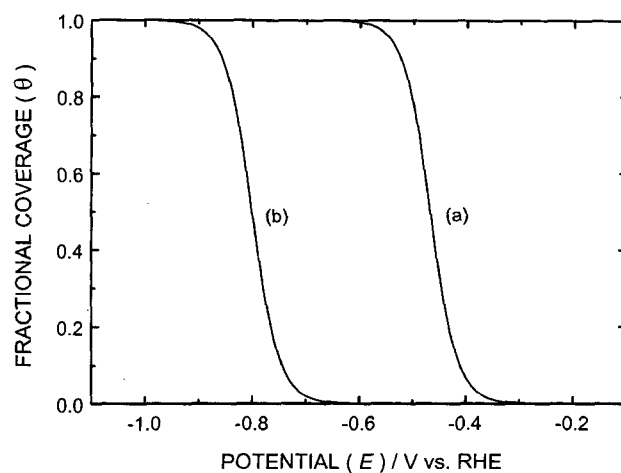


Fig. 12. The numerically calculated Langmuir adsorption isotherm ( $\theta$  vs.  $E$ ) at the poly-Pt/0.5 M LiOH aqueous electrolyte interface. (a)  $K = 2.7$  (UPD H) and (b)  $K = 6.2 \times 10^{-6}$  (OPD H).

Table 2. The measured phase shift ( $-\phi$ ) for the optimum intermediate frequency (ca. 13 Hz) and the estimated fractional surface coverage ( $\theta$ ) at the poly-Pt/0.5 M LiOH aqueous electrolyte interface

$E$ (V vs. RHE)	$-\phi$ (deg)	$\theta^a$
-0.26	84.1	$\approx 0$
-0.31	83.9	0.002
-0.36	81.4	0.033
-0.41	72.1	0.145
-0.46	54.1	0.364
-0.51 <sup>b</sup>	58.3	0.313
-0.71 <sup>b</sup>	74.5	0.116
-0.76	67.8	0.198
-0.81	38.7	0.550
-0.86	15.4	0.833
-0.91	7.0	0.935
-0.96	3.4	0.978
-1.01	2.0	0.995
-1.06	1.6	$\approx 1$

<sup>a</sup> Estimated using the measured phase shift ( $-\phi$ ).

<sup>b</sup> Transition between the UPD H and the OPD H.

respectively. As expected, Table 2, Figs. 10, and 11 also show that the  $-\phi$  vs.  $E$  corresponds well to the  $\theta$  vs.  $E$  at the interface. Table 2, Figs. 10, and 11 are obtained through the previously described procedures. In Figs. 10 and 11, the regions (a) and (b) correspond to the UPD H and the OPD H regions, respectively. It should be noted that the Langmuir adsorption isotherm of the UPD H shown in Fig. 11(a) is located the region of the UPD H peaks on the cyclic voltammogram shown in Fig. 9 and the corresponding cathode potentials shown in Table 2. On the other hand, the Langmuir adsorption isotherm of the OPD H shown in Fig. 11(b) is located beyond the UPD H peaks (ca. -0.381 and -0.517 V

vs. RHE) on the cyclic voltammogram and the corresponding cathode potentials.

Figure 12 shows the numerically calculated Langmuir adsorption isotherms ( $\theta$  vs.  $E$ ) corresponding to the two different values of  $K$  or  $\Delta G_{ads}$  shown in Fig. 11. Fig. 12 also shows that the transition region (-0.484 to -0.709 V vs. RHE) shown in Fig. 11 and Table 2 is related to the overlapped region between the Langmuir adsorption isotherm (a), i.e., the UPD H region, and the Langmuir adsorption isotherm (b), i.e., the OPD H region. It implies that the processes of the UPD H and the OPD H for the cathodic HER at the poly-Pt electrode interface proceed independently of each other. In other words, the UPD H and the OPD H are the independent processes depending on the adsorption sites of H rather than the sequential processes for the cathodic HER. However, as expected, the value of  $K$  of the UPD H is much ( $\sim 10^5$ - $10^7$  times) greater than that of the OPD H.<sup>7,8,23)</sup> It implies that only the OPD H can contribute to the cathodic HER.

Under the Langmuir adsorption conditions,<sup>48)</sup> the transition region implies that the equilibrium constant ( $K$ ) for H adsorption and the standard free energy ( $\Delta G_{ads}$ ) of H adsorption shift depending on the applied dc potential ( $E$ ), i.e., the cathode potential. In other words, the poly-Pt electrode surface has the two distinct adsorption sites of the UPD H and the OPD H corresponding to the two different values of  $K$  or  $\Delta G_{ads}$ . Figs. 11 and 12 show that  $K$  transits from 2.7 (UPD H) to  $6.2 \times 10^{-6}$  (OPD H) depending on  $E$  and vice versa. Similarly, Figs. 11, 12, and Eq. (6) show that  $\Delta G_{ads}$  transits from -2.5 kJ/mol (UPD H) to 29.7 kJ/mol (OPD H) depending on  $E$  and vice versa. A minus sign of  $\Delta G_{ads}$  implies that the exothermic reaction occurs at the UPD H region. In other words, the process of the UPD H is spontaneous at the interface. Consequently, it can be interpreted that the UPD H and the OPD H on the adsorption sites of the poly-Pt surface act as two distinguishable electroadsorbed H species. The criterion of the UPD H and the OPD H is the H adsorption sites and

**Table 3. The electrode kinetic and thermodynamic parameters for the potential ranges at the poly-Pt and the Pt(100)/0.5 M H<sub>2</sub>SO<sub>4</sub> and 0.5 M LiOH aqueous electrolyte interfaces**

Electrode/Electrolyte	UPD H	OPD H
	$K$	$K$
	$\Delta G_{ads}$ (kJ/mol)	$\Delta G_{ads}$ (kJ/mol)
poly-Pt/0.5 M H <sub>2</sub> SO <sub>4</sub>	-	$2.1 \times 10^{-4}$
	-	21.0
Pt(100)/0.5 M H <sub>2</sub> SO <sub>4</sub> *	-	$1.5 \times 10^{-4}$
	-	21.8
poly-Pt/0.5 M LiOH	2.7	$6.2 \times 10^{-6}$
	-2.5	29.7
Pt(100)/0.5 M LiOH *	1.9	$6.1 \times 10^{-6}$
	-1.6	29.7

\* Commercially prepared single-crystal disc. Ref. 23.

processes rather than the H<sub>2</sub> evolution reactions and potentials.

### 3.5. Comparison of the electrode kinetic and thermodynamic parameters

Table 3 shows the electrode kinetic and thermodynamic parameters ( $K$ ,  $\Delta G_{ads}$ ) for the potential ranges (0.241 to -0.209 V vs. RHE for the 0.5 M H<sub>2</sub>SO<sub>4</sub> and to -1.109 V vs. RHE for the 0.5 M LiOH) at the poly-Pt and the Pt(100)/0.5 M H<sub>2</sub>SO<sub>4</sub> and 0.5 M LiOH aqueous electrolyte interfaces.<sup>23)</sup> It suggests that the difference of  $K$  and  $\Delta G_{ads}$  between the poly-Pt wire and the Pt(100) disc electrodes can be neglected. As previously described, it implies that the poly-Pt wire mostly consists of the same single-crystal face (100) substrates. It also implies that  $K$  and  $\Delta G_{ads}$  depend strongly on the H adsorption sites on the single-crystal face (100) of the poly-Pt surface rather than the orientation and size of grains, i.e., small crystalline zones, on the poly-Pt surface. However, it should be noted that the preparation of the Pt(100) disc electrode is more difficult than that of the poly-Pt wire electrode. As expected, the Pt(100) disc is several times expensive than the poly-Pt wire.<sup>51)</sup> On a viewpoint of the cost and efficiency, the use of the poly-Pt wire electrode is more effective and reasonable for the cathodic HER at the interfaces.

### 3.6. Comment on the existing thermodynamic results

The comparison of the obtained experimental data and the existing thermodynamic results is important and necessary to confirm the validity and significance of the phase-shift method for the Langmuir adsorption isotherms of the UPD H and the OPD H. For the Ni electrode interfaces, the experimental data presented using the phase-shift method for the Frumkin adsorption isotherm of the OPD H correspond well to the existing electrode kinetic and thermodynamic results for the OPD H.<sup>26)</sup>

The relation between the UPD H and the OPD H at the Pt electrode interfaces, on a thermodynamic basis, has been intensively studied by Jerkiewicz *et al.*<sup>6-8,12,13,15,16,49,50)</sup> As pointed out by Jerkiewicz *et al.*,<sup>15)</sup> the existing thermodynamic

results are determined on the basis of the general electrochemical adsorption isotherm rather than the Langmuir or the Frumkin adsorption isotherm. In addition, it should be noted that the prepared single-crystal Pt(100) electrodes are perfect and so they have homogeneous surfaces. Also, it should be noted that the form of the Langmuir adsorption isotherm depends strongly on the fractional surface coverage rather than the lateral interaction effect.<sup>4,10,18,21,23,40,49,50)</sup> However, as shown in Fig. 8 and Table 1, the endothermic reaction, i.e.,  $\Delta G_{ads} > 0$ , occurs at the OPD H region. As previously described, it implies that the adsorption process of the OPD H on the adsorption sites of the poly-Pt electrode surface needs 21.0 kJ/mol. Therefore, it is easily understood that the obtained experimental data, i.e.,  $\Delta G_{ads}$  of the OPD H: 21.0 kJ/mol for  $K = 2.1 \times 10^{-4}$ , shown in Fig. 8 and Table 3 are well complementary to the existing thermodynamic results, i.e.,  $\Delta G_{ads}$  of the UPD H: -22 to -9 kJ/mol or -25 to -12 kJ/mol, shown in Refs. 7 and 8. It should be noted that the exothermic reaction, i.e.,  $\Delta G_{ads} < 0$ , occurs at the UPD H region. In other words, the UPD H on the adsorption sites of the Pt(100) electrode surface is the spontaneous adsorption process.

For example, it is readily calculated using Eq. (6) that  $K$  is  $7.2 \times 10^3$  for  $\Delta G_{ads} = -22$  kJ/mol (UPD H) and is 37.8 for  $\Delta G_{ads} = -9$  kJ/mol (UPD H). Figs. 13(a), (b), and (c) show the Langmuir adsorption isotherms ( $\theta$  vs.  $E$ ) corresponding to the existing thermodynamic results ( $K = 7.2 \times 10^3$  for  $\Delta G_{ads} = -22$  kJ/mol and  $K = 37.8$  for  $\Delta G_{ads} = -9$  kJ/mol) and the obtained experimental data ( $K = 2.1 \times 10^{-4}$  for  $\Delta G_{ads} = 21.0$  kJ/mol), respectively. In contrast to the nebulous thermodynamic distinction between the UPD H and the OPD H,<sup>49,50)</sup> the Langmuir adsorption distinction between the UPD H and the OPD H is plotted clearly as shown in Fig. 13 as well as Figs. 11 and 12. However, it should be noted that the Langmuir adsorption isotherms of the UPD H shown in Figs. 13(a) and (b) are located the region of the UPD H peaks on the cyclic voltammogram shown in Fig. 1. It implies that  $K$

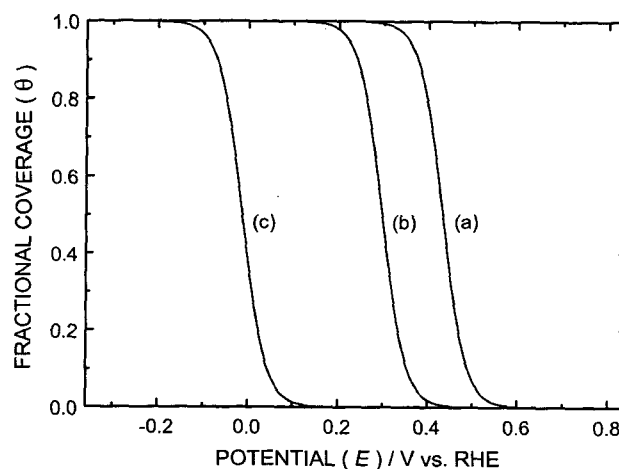


**Fig. 13. The numerically calculated Langmuir adsorption isotherm ( $\theta$  vs.  $E$ ) at the Pt/0.5 M H<sub>2</sub>SO<sub>4</sub> aqueous electrolyte interfaces. (a)  $K = 7.2 \times 10^3$  (UPD H), (b)  $K = 37.8$  (UPD H),<sup>7,8)</sup> and (c)  $K = 2.1 \times 10^{-4}$  (OPD H).**

of the UPD H is much greater than that of the OPD H at the interfaces. Also, it implies that the experimental data presented using the phase-shift method and related discussions are reasonable and valid at the interfaces.

As shown in Figs. 11 and 12, Fig. 13 also shows that the UPD H and the OPD H are the independent processes depending on the H adsorption sites of the poly-Pt surface rather than the sequential processes for the cathodic HER. Considering the independent processes of the UPD H and OPD H, i.e., the two different adsorption sites of the UPD H and the OPD H, the superposition or the extension between the Langmuir adsorption isotherms of the UPD H and the OPD H cannot be occurred at the cathode potential range. Therefore, as expected, the overlapped region between the Langmuir adsorption isotherms of the UPD H and the OPD H must be occurred as shown in Figs. 12 and 13.

Taking into account the phase-shift profile for the optimum intermediate frequency based on the Frumkin adsorption isotherm,<sup>19,25,26)</sup> the two different adsorption sites of the UPD H and the OPD H,<sup>21,23)</sup> the high activity of the adsorption sites of the UPD H,<sup>7,8,48)</sup> the nebulous thermodynamic distinction between the UPD H and the OPD H,<sup>49,50)</sup> and the nature of the anions at the Pt/0.5 M H<sub>2</sub>SO<sub>4</sub> aqueous electrolyte interfaces,<sup>7,8,12,13,15,17)</sup> it can be explained that  $\theta$  of the UPD H has reached unity already at the onset of the OPD H as shown in Figs. 12 and 13. Of course, as previously described, there is neither the superposition nor the extension between the Langmuir adsorption isotherms of the UPD H and the OPD H at the cathode potential range. It can also be confirmed by referring to Figs. 11-13. Consequently, it can be interpreted that the Langmuir adsorption isotherm shown in Fig. 8 is attributed to the OPD H for the cathodic HER. The experimental data presented using the phase-shift method for the OPD H are well complementary to the existing thermodynamic results for the UPD H.

The thermodynamic distinction between the H<sup>+</sup> and the anionic adsorption effects on the adsorption sites of the UPD H at the poly-Pt/0.5 M H<sub>2</sub>SO<sub>4</sub> electrolyte interface cannot be presented using the phase-shift method. Since, the adsorption processes of the UPD H and the anions are superimposed at the cathode potential range. On the other hand, as shown in Figs. 11, 12, and Table 3, the thermodynamic distinction between the UPD H and the OPD H at the poly-Pt/0.5 M LiOH electrolyte interface can be expressed in terms of  $\Delta G_{ads}$ , i.e.,  $K$  described in Eq. (6). However, it should be noted that  $\Delta G_{ads}$  ( $K$ ) depends strongly on the adsorption sites of the UPD H and the OPD H on the poly-Pt surface. Finally, to evaluate the behaviors of the UPD H, the OPD H, and the adsorbed anions on temperature ( $T$ ) variation,<sup>12,13)</sup> the temperature dependent study on the UPD H, the OPD H, and the adsorbed anions at the interfaces might be supplemented using the phase-shift method.

#### 4. Conclusions

The phase-shift method for the Langmuir adsorption isotherms of the UPD H and the OPD H for the cathodic HER

is proposed. The simplified equivalent circuit for the optimum intermediate frequency and the corresponding phase-shift equation are well fitted to the poly-Pt/0.5 M H<sub>2</sub>SO<sub>4</sub> and 0.5 M LiOH aqueous electrolyte interfaces regardless of H<sub>2</sub> evolution. The behavior of the phase shift ( $0^\circ \leq -\phi \leq 90^\circ$ ) for the optimum intermediate frequency corresponds well to that of the fractional surface coverage ( $1 \geq \theta \geq 0$ ) at the interfaces. The phase-shift profile ( $-\phi$  vs.  $E$ ) for the optimum intermediate frequency, i.e., the phase-shift method, can be used as a new electrochemical method to determine the Langmuir adsorption isotherm ( $\theta$  vs.  $E$ ) of the UPD H and the OPD H for the cathodic HER at the interfaces. At the poly-Pt/0.5 M H<sub>2</sub>SO<sub>4</sub> aqueous electrolyte interface, the equilibrium constant ( $K$ ) and the standard free energy ( $\Delta G_{ads}$ ) of the OPD H are  $2.1 \times 10^{-4}$  and 21.0 kJ/mol, respectively. At the poly-Pt/0.5 M LiOH aqueous electrolyte interface,  $K$  transits from 2.7 (UPD H) to  $6.2 \times 10^{-6}$  (OPD H) depending on  $E$  and vice versa. Similarly,  $\Delta G_{ads}$  transits from -2.5 kJ/mol (UPD H) to 29.7 kJ/mol (OPD H) depending on  $E$  and vice versa. The transition of  $K$  and  $\Delta G_{ads}$  is attributed to the two distinct adsorption sites of the UPD H and the OPD H on the poly-Pt surface. The UPD H and the OPD H on the adsorption sites of the poly-Pt surface act as two distinguishable electroadsorbed H species. The UPD H and the OPD H are the independent processes depending on the H adsorption sites of the poly-Pt surface rather than the sequential processes for the cathodic H<sub>2</sub> evolution reactions at the poly-Pt interface. The criterion of the UPD H and the OPD H is the H adsorption sites and processes rather than the H<sub>2</sub> evolution reactions and potentials. The electrode kinetic and thermodynamic parameters ( $K$ ,  $\Delta G_{ads}$ ) depend strongly on the H adsorption sites of the poly-Pt surface. The poly-Pt wire electrode is more efficient and useful than the Pt(100) disc electrode for the cathodic H<sub>2</sub> evolution reactions in the aqueous electrolytes. The phase-shift method is well complementary to the thermodynamic method rather than conflicting.

#### Acknowledgements

The authors thank Dr. Mu. S. Cho (The First President of Kwangwoon University, Seoul, Korea) for supporting the EG&G PAR 273A Potentiostat/Galvanostat, Schlumberger SI 1255 HF FRA, and software packages. The authors also thank Professor G. Jerkiewicz (Universite de Sherbrooke, Quebec, Canada) for his valuable suggestions and encouragement on the phase-shift method.

#### References

1. S. Trasatti, In "Advances in Electrochemical Science and Engineering", H. Gerischer and C. T. Tobias, Editors, Vol. 2, pp. 1-85, VCH, New York (1993).
2. J. Lipkowski and P. N. Ross, Editors, "Structure of Electrified Interfaces", VCH, New York (1993).
3. E. Gileadi, "Electrode Kinetics", pp. 164-169, VCH, New York (1993).
4. B. E. Conway and G. Jerkiewicz, Editors, "Electrochemistry and Materials Science of Cathodic Hydrogen Absorption and

- Adsorption", PV 94-21, The Electrochemical Society, Pennington, NJ (1995).
5. D. M. Kolb, *Prog. Surf. Sci.*, **51**, 109 (1996).
  6. G. Jerkiewicz and A. Zolfaghari, *J. Electrochem. Soc.*, **143**, 1240 (1996).
  7. A. Zolfaghari, F. Villiard, M. Chayer, and G. Jerkiewicz, *J. Alloys Compounds*, **253-4**, 481 (1997).
  8. G. Jerkiewicz, *Prog. Surf. Sci.*, **57**, 137 (1998).
  9. M. W. Breiter, G. Staikov, and W. J. Lorenz, In "Electrochemistry and Materials Science of Cathodic Hydrogen Absorption and Adsorption", B. E. Conway and G. Jerkiewicz, Editors, PV 94-21, pp. 152-166, The Electrochemical Society, Pennington, NJ (1995).
  10. D. A. Harrington and B. E. Conway, *Electrochim. Acta*, **32**, 1703 (1987).
  11. J. Barber, S. Morin, and B. E. Conway, *J. Electroanal. Chem.*, **446**, 125 (1998).
  12. G. Jerkiewicz and A. Zolfaghari, *J. Phys. Chem.*, **100**, 8454 (1996).
  13. A. Zolfaghari, M. Chayer, and G. Jerkiewicz, *J. Electrochem. Soc.*, **144**, 3034 (1997).
  14. S. Morin, H. Dumont, and B. E. Conway, *J. Electroanal. Chem.*, **412**, 39 (1996).
  15. A. Zolfaghari and G. Jerkiewicz, *J. Electroanal. Chem.*, **467**, 177 (1999).
  16. G. Jerkiewicz and A. Zolfaghari, In "Electrochemistry and Materials Science of Cathodic Hydrogen Absorption and Adsorption", B. E. Conway and G. Jerkiewicz, Editors, PV 94-21, pp. 31-43, The Electrochemical Society, Pennington, NJ (1995).
  17. B. E. Conway, In "Interfacial Electrochemistry", A. Wieckowski, Editor, pp. 131-150, Marcel Dekker, New York (1999).
  18. E. Gileadi, In "Electrosorption", E. Gileadi, Editor, pp. 1-18, Plenum Press, New York, (1967).
  19. J. H. Chun and K. H. Ra, *J. Electrochem. Soc.*, **145**, 3794 (1998).
  20. J. H. Chun and C. D. Cho, *J. Korean Electrochem. Soc.*, **2**, 213 (1999).
  21. J. H. Chun and K. H. Ra, In "Hydrogen at Surfaces and Interfaces", G. Jerkiewicz, J. M. Feliu, and B. N. Popov, Editors, PV 2000-16, pp. 159-173, The Electrochemical Society, Pennington, NJ (2000).
  22. J. H. Chun, K. H. Mun, and C. D. Cho, *J. Korean Electrochem. Soc.*, **3**, 25 (2000).
  23. J. H. Chun, K. H. Ra, and N. Y. Kim, *Int. J. Hydrogen Energy*, **26**, 941 (2001).
  24. J. H. Chun and S. K. Jeon, *J. Korean Electrochem. Soc.*, **4**, 118 (2001).
  25. J. H. Chun and S. K. Jeon, *J. Korean Electrochem. Soc.*, **4**, 146 (2001).
  26. J. H. Chun, K. H. Ra, and N. Y. Kim, *J. Electrochem. Soc.*, **149**, E325 (2002).
  27. E. Gileadi, E. Kirowa-Eisner, and J. Penciner, "Interfacial Electrochemistry", pp. 6-13, 72-73, 311-312, Addison-Wesley, Reading, MA (1975).
  28. D. M. Macarthur, In "Characterization of Solid Surfaces", P. F. Kane and G. B. Larrabee, Editors, pp. 181-201, Plenum Press, New York (1978).
  29. F. T. Wagner and P. N. Ross, *J. Electroanal. Chem.*, **150**, 141 (1983).
  30. J. Jiang and A. Kucernak, *Electrochem. Solid-State Lett.*, **3**, 559 (2000).
  31. E. Gileadi, "Electrode Kinetics", pp. 287-289, VCH, New York (1993).
  32. A. Zolfaghari and G. Jerkiewicz, In "Electrochemical Surface Science of Hydrogen Adsorption and Absorption", G. Jerkiewicz and P. Marcus, Editors, PV 97-16, pp. 133-158, The Electrochemical Society, Pennington, NJ (1997).
  33. J. Clavilier, In "Interfacial Electrochemistry", A. Wieckowski, Editor, pp. 231-248, Marcel Dekker, New York (1999).
  34. N. M. Markovic and P. N. Ross, In "Interfacial Electrochemistry", A. Wieckowski, Editor, pp. 821-841, Marcel Dekker, New York (1999).
  35. E. Gileadi, "Electrode Kinetics", pp. 287-291, VCH, New York (1993).
  36. E. Gileadi, E. Kirowa-Eisner, and J. Penciner, "Interfacial Electrochemistry", pp. 86-93, Addison-Wesley, Reading, MA (1975).
  37. D. D. MacDonald, "Transient Techniques in Electrochemistry", pp. 298-303, Plenum Press, New York (1977).
  38. J. R. Scully, D. C. Silverman, and M. W. Kendig, Editors, "Electrochemical Impedance: Analysis and Interpretation", ASTM, Philadelphia, PA (1993).
  39. E. Gileadi, "Electrode Kinetics", pp. 293-303, VCH, New York (1993).
  40. S. Sarangapani, B. V. Tilak, and C. P. Chen, *J. Electrochem. Soc.*, **143**, 3791 (1996).
  41. S. S. Buttarello, G. Tremiliosi-Filho, E. R. Gonzalez, In "Electrochemistry and Materials Science of Cathodic Hydrogen Absorption and Adsorption", B. E. Conway and G. Jerkiewicz, Editors, PV 94-21, pp. 299-312, The Electrochemical Society, Pennington, NJ (1995).
  42. R. D. Armstrong and M. Henderson, *J. Electroanal. Chem.*, **39**, 81 (1972).
  43. J. G. Holbrook, "Laplace Transforms for Electronic Engineers", pp. 141-146, Pergamon Press, New York (1959).
  44. E. Gileadi and B. E. Conway, In "Modern Aspects of Electrochemistry", JOM. Bockris and B. E. Conway, Editors, Vol. 3, Chap. 5, Butterworth, Washington, DC (1964).
  45. E. Gileadi, "Electrode Kinetics", pp. 307-318, VCH, New York (1993).
  46. A. K. N. Reddy, In "Electrosorption", E. Gileadi, Editor, pp. 53-71, Plenum Press, New York (1967).
  47. A. J. Apple, In "Comprehensive Treatise of Electrochemistry", B. E. Conway, JOM. Bockris, E. Yeager, S. U. M. Khan, and R. E. White, Editors, Vol. 7, pp. 218-228, Plenum Press, New York (1983).
  48. E. Gileadi, "Electrode Kinetics", pp. 261-271, VCH, New York (1993).
  49. B. E. Conway and G. Jerkiewicz, *Electrochim. Acta*, **45**, 4075 (2000).
  50. B. E. Conway and G. Jerkiewicz, In "Hydrogen at Surfaces and Interfaces", G. Jerkiewicz, J. M. Feliu, and B. N. Popov, Editors, PV 2000-16, pp. 1-11, The Electrochemical Society, Pennington, NJ (2000).
  51. "Alfa Aesar Research Chemicals, Metals, and Materials", pp. 1003-1010, Johnson Matthey Co., Ward Hill, MA (1999-2000).